Steel and Composite Structures, Vol. 10, No. 2 (2010) 187-205
DOI: http://dx.doi.org/10.12989/scs.2010.10.2.187

Behaviors of concrete filled square steel tubes confined by carbon fiber sheets (CFS) under compression and cyclic loads

Park, Jai Woo[1], Hong, Young Kyun[2] and Choi, Sung Mo[3]*

[1]*University of Seoul, Department of Architecture Engineering, Seoul, Korea.*
[2]*Hongik University, Department of Architecture, Seoul, Korea.*
[3]*University of Seoul, Department of Architecture Engineering, Seoul, Korea.*

(Received September 3, 2009, Accepted March 18, 2010)

Abstract. The existing CFT columns present the deterioration in confining effect after the yield of steel tube, local buckling and the deterioration in load capacity. If lateral load such as earthquake load is applied to CFT columns, strong shearing force and moment are generated at the lower part of the columns and local buckling appears at the column. In this study, axial compression test and beam-column test were conducted for existing CFT square column specimens and those reinforced with carbon fiber sheets (CFS). The variables for axial compression test were width-thickness ratio and the number of CFS layers and those for beam-column test were concrete strength and the number of CFS layers. The results of the compression test showed that local buckling was delayed and maximum load capacity improved slightly as the number of layers increased. The specimens' ductility capacity improved due to the additional confinement by carbon fiber sheets which delayed local buckling. In the beam-column test, maximum load capacity improved slightly as the number of CFS layers increased. However, ductility capacity improved greatly as the increased number of CFS layers delayed the local buckling at the lower part of the columns. It was observed that the CFT structure reinforced with carbon fiber sheets controlled the local buckling at columns and thus improved seismic performance. Consequently, it was deduced that the confinement of CFT columns by carbon fiber sheets suggested in this study would be widely used for reinforcing CFT columns.

Keywords: concrete filled steel tube; CFT, composite column; confining effect; carbon fiber sheet.

1. Introduction

The necessity of a new structural system applicable to huge buildings has emerged along with the increase of high-rise large-scale buildings. For this reason, composite structures have received increasing attention in which more than two materials complement each other to provide dynamically excellent performance. CFT column is one of these composite members in which the tensile strength of steel tube and compressive strength of concrete complement each other. The concrete filled inside the steel tube delays the local buckling at the steel tube and improves ductility capacity (Fukumoto 2005). Especially, the concrete filled inside circular steel tube features 3-axis-stress, which improves the compressive strength of the column. Thanks to this structural superiority, CFT columns are widely used for bridge piers as well as skyscrapers' columns (Tao *et al*. 2008).

Kang *et al.* (2001) conducted axial compression test for CFT square columns under central axial load

* Corresponding author, Professor, E-mail: smc@uos.ac.kr

with the variable of non-filling, width-thickness ratio and concrete strength. The results showed that CFT columns exhibited the increase in maximum load capacity, proving that they are superior to hollow steel tube columns. However, the deterioration in load capacity and presentation of local buckling at the steel tube were observed after maximum load capacity, which was followed by failure.

Choi *et al.* (2000) conducted the test for CFT square columns under low axial load and cyclic horizontal force simultaneously. The variables in the test to examine maximum load capacity, initial stiffness and deformation were width-thickness ratio, concrete strength and concrete-filling. Local buckling was observed at the lower part of the columns after maximum load capacity and local buckling expanded as load capacity deteriorated.

A variety of reinforcements have been suggested to solve the problem of local buckling on existing CFT columns. Ge and Usami(1992) decided to weld steel strips to the inner surface of column to delay local buckling Fig. 1 (a) and Lin *et al.* (1993) suggested welding shear studs to the inner surface of column Fig. 1 (b). In addition, Huang and Yeh (2002) proposed to attach tied bars at the corners inside column Fig. 1 (c) and Cai and He (2006) suggested having binding bars pass through column to be attached inside it Fig. 1 (d).

However, these ideas for reinforcement require welding stiffeners inside column and thus are associated with difficulty in construction workability. Moreover, having the stiffeners penetrate columns can change material properties and exert negative influence on the load capacity of members.

Previously in construction engineering, reinforcement with additional layer of steel plate was employed to mitigate the failure at the lower part of columns caused by cyclic lateral load(Boyd 1995, Xiao and Choi 2002). Stiffeners or steel plates were used to mitigate local buckling at the lower part of CFT columns. However, reinforcement with steel plates has drawbacks such as increased weight due to the additional layer of steel plate, complicated process, changes in material property due to steel plate welding and deteriorated durability against climatic changes. The necessity of new reinforcement materials has emerged in order to solve these problems. In an attempt to deal with these problems, reinforcement with carbon fiber sheets is widely used. Greater tensile strength than steel plate, convenience in construction and maintained material property thanks to welding-free process are the main reasons carbon fiber sheets are widely used as reinforcement material (Teng *et al*. 2001).

Previously in study for FRP sheets, Xiao and He(2000) carried out compression test for circular concrete cylinders confined with carbon fiber sheets. It was observed that the confining effect of carbon fiber sheets led to the increase compression strength of concrete.

Saadatmanesh *et al*. (1996) conducted cyclic lateral load test for R/C circular columns by confining the potential plastic hinge area of the lower part of the columns by carbon fiber sheets. The results showed that additional confinement by carbon fiber not only sheets improved strength and ductility, but

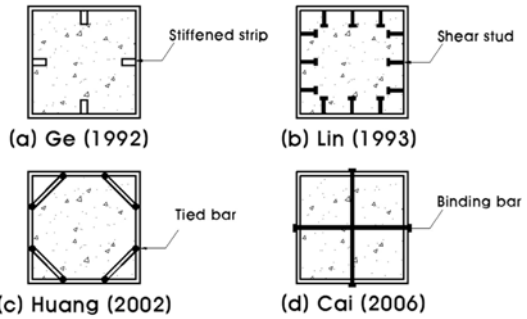

Fig. 1 Stiffner reinforced CFT section details

also delayed failure and mitigated load capacity deterioration after maximum load capacity.

Thus, carbon fiber sheets are expected to be widely used as reinforcement material to improve the performance of existing members.

As mentioned above, great shearing force and moment generated at the lower part of CFT columns due to horizontal load such as earthquake load cause local buckling(Sakino and Tommi 1981). So, it is required to reinforce the columns to control local buckling.

Xiao *et al.* (2005) conducted an experimental study on compressive strength and flexural rigidity of CFT columns confined by carbon fiber sheets to deal with the local buckling at the column. Horizontal load such as earthquake load applied to CFT columns causes local buckling at the lower part of the columns and failure. In order to solve this problem, Xiao *et al.* (2005) confined the lower part of CFT circular columns by carbon fiber sheets and carried out flexural test using the concept shown in Fig. 1. The results of the compression test revealed that additional confinement by carbon fiber sheets delayed local buckling and improved compressive strength by 54%~136% depending on the number of CFS layers. As regards flexural rigidity, the delay in local buckling led to improvement in ductility capacity and energy dissipation and thus improved seismic performance.

Tao *et al.* (2007) conducted fire-resistance test for CFT square and circular columns to display the advantages associated with the confinement by carbon fiber sheets to reinforce the columns. And, he carried out an experimental study on the performance of the confinement by carbon fiber sheets under compressive force and eccentric axial load. The experiment proved that reinforcement with carbon fiber sheets improved load capacity and ductility capacity.

In construction field, CFT square columns are more commonly used than CFT circular columns. It is because CFT square columns are superior to circular columns in terms of construction process at connections and ductility thanks to larger amount of steel at the outermost angle. Consequently, CFT square columns have been chosen as the main object of the test and analysis in this study.

An experimental study was conducted on the compressive behavior and performance of CFT square columns confined by carbon fiber sheets. Column test was conducted with the variables of width-thickness ratio (B/t) and the number of CFS layers for the columns under central axial load. Beam-column test was also carried out with variables of concrete strength and the number of CFS layers under low axial load and cyclic horizontal load. After the tests with 17 specimens, the destructive behavior, maximum load capacity and ductility capacity of CFT columns and those confined by carbon fiber sheets were compared and analyzed.

2. Compression test

Most of central axial load is applied to columns, which are compression members. This chapter covers the results of central axial load test conducted for CFT columns and those confined by carbon fiber sheets. With the variables of width-thickness ratio(B/t) and the number of CFS layers, destructive behavior, load capacity and ductility capacity of CFT columns and those confined by carbon fiber sheets were compared and analyzed.

2.1 Plan for specimens and variables

2.1.1 Fabrication of specimens and test variables

For central axial load test, nine specimens were fabricated with SS 400 steel by casting concrete in

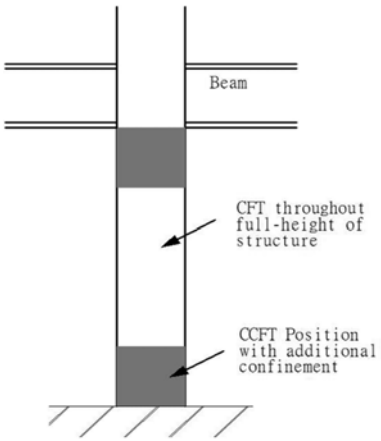

Fig. 2 The concept of CCFT column

square steel tubes which were 125×125×3.2, 4.5 and 6.0 (mm) in sizes and 550 (mm) in length. As shown in Fig. 2, carbon fiber sheets with the layered length of 10 cm reinforced the shear plane of the columns in the direction of width. Table 1 shows the plan for the specimens and variables. The variables for the test were width-thickness ratio and the number of CFS layers. In order to find the influence of width-thickness ratio, the specimens were fabricated in the width-thickness ratio of 21~39. The numbers of CFS layers confining the CFT columns were zero, one and three in the test for comparing and analyzing the behavior of the columns.

2.1.2 Material test

The design strength and compressive strength of the concrete were 50 MPa and 49.9 MPa, respectively. The yield strength and tensile strength of 3.2 mm, 4.5 mm and 6.0 mm steel were 304, 300 and 324 MPa and 344, 384 and 394 MPa, respectively. The design thickness and tensile strength of the carbon fiber sheets provided by the manufacturer were 0.111 mm and 3500 MPa, respectively.

2.1.3 Specimen setting

Central axial load was applied to the specimens with a 3,000kN UTM as shown in Fig. 3. The

Table 1 Plan for specimens and variables

Specimen	Size (mm)	B/t ratio	L/B ratio	f'_c (MPa)	f_y (MPa)	CFS Layer	$A_s/A_{con'c}$ (%)	A_s (mm^2)	$A_{con'c}$ (mm^2)
R3N	125×125×3.2	39	4.4	49.9	326	0	9.37	1,464	14,161
R3F-1	125×125×3.2	39	4.4	49.9	326	1	9.37	1,464	14,161
R3F-3	125×125×3.2	39	4.4	49.9	326	3	9.37	1,464	14,161
R4N	125×125×4.5	28	4.4	49.9	373	0	13.88	2,169	13,456
R4F-1	125×125×4.5	28	4.4	49.9	373	1	13.88	2,169	13,456
R4F-3	125×125×4.5	28	4.4	49.9	373	3	13.88	2,169	13,456
R6N	125×125×6.0	21	4.4	49.9	311	0	18.28	2,856	12,769
R6F-1	125×125×6.0	21	4.4	49.9	311	1	18.28	2,856	12,769
R6F-3	125×125×6.0	21	4.4	49.9	311	3	18.28	2,856	12,769

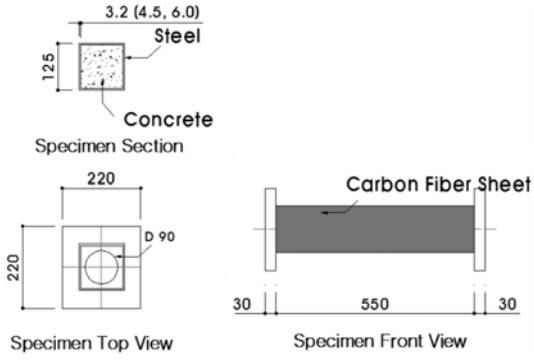

Fig. 3 Fabrication of the specimens (Column test)

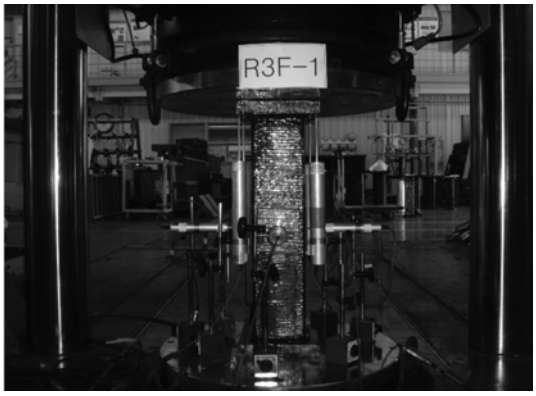

Fig. 4 Test setup (Compression Test)

specimens were installed inside the UTM and the load was applied to the steel surface and concrete surface simultaneously.

In order to observe the axial displacement of the specimens, 4 LVDTs were mounted on the edges of the endplate.

2.2 Failure mode and Load-Axial displacement curves

2.2.1 Destructive behavior procedures

As shown in Fig. 5, the steel tubes of specimens were bent at 15~30 cm point from the bottom end of the columns followed by local buckling and failure. In existing CFT columns, local buckling was presented at the central part of the steel tube at an early stage of loading and it expanded as loading intensified. CFT columns reinforced with carbon fiber sheets exhibited the similar behavior as the existing CFT columns. As loading intensified, local buckling expanded and carbon fiber sheets were ripped followed by rupture. Local buckling was observed at one spot at 4 specimens (R3F-1, R6N, R6F-1 and R6F-3) and two spots at the other 5 specimens.

In R3N specimen with width-thickness ratio of 39, local buckling was presented at 15 cm point from the bottom end of the column at the axial displacement of 3.7 mm. As local buckling expanded,

Fig. 5 Failure modes of the specimens

additional buckling was observed at 10 cm point from the bottom end of the column at the axial displacement of 5.5 mm followed by specimen failure. R3F specimen reinforced with 3 carbon fiber sheets exhibited inflation at 20 cm point from the bottom end of the column at the axial displacement of 5.8 mm, but carbon fiber sheets were not ruptured. The rupture of the sheets started at the axial displacement of 8.7 mm and local buckling was observed at 10 cm point from the bottom end of the column at axial displacement of 12 mm followed by failure.

2.2.2 Load-displacement relations

The average of the axial displacements measured by the 4 LVDTs mounted on each specimen in the longitudinal direction of column was used as axial displacement. In existing CFT columns, rapid deterioration in load capacity was observed after maximum load capacity and axial displacement increased without the deterioration in load capacity as constant deformation progressed.

In CFT columns reinforced with carbon fiber sheets, the decrease in load capacity started at the point on load-displacement curves when the carbon fiber sheets were ripped. The buckling at the CFT columns expanded due to the increase in axial load and the ripped area expanded. Load capacity started to deteriorate at the point when the carbon fiber sheets were ripped. Unlike the case of the existing CFT columns, load capacity deterioration was gradual. In R6F-3 specimen with the width-thickness ratio of 21, while loading increased continuously along with axial displacement, the carbon fiber sheets were ripped at the axial displacement of 10 mm followed by the rapid deterioration in load capacity.

Fig. 6 and 7 show the load-displacement curves and failure shape of the existing CFT columns (RN specimens) and those reinforced with 3 carbon fiber sheets (RF-3 specimens), respectively.

2.3 Analysis of column test results

Table 3 shows not only the load capacity (P_u) and displacement (δ_u) at failure point, but also the load capacity (P_y) and displacement (δ_y) at yield point. Maximum load capacity (P_{max}) and ductility capacity(DI) are also shown in table 3. Yield point was decided by the 1/3 tangent method(Choi, 2000) and failure point (δ_u) was defined as the point of 10% deterioration of load capacity from maximum load capacity(Varma *et al*. 2004). Ductility capacity of the specimens is defined as Eq. (1).

$$DI = \frac{\delta_u}{\delta_y} \tag{1}$$

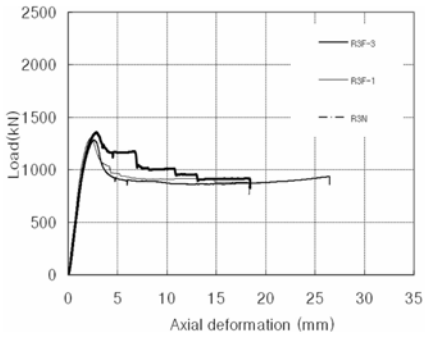

(a) Load-Displacement curves of R3 specimens

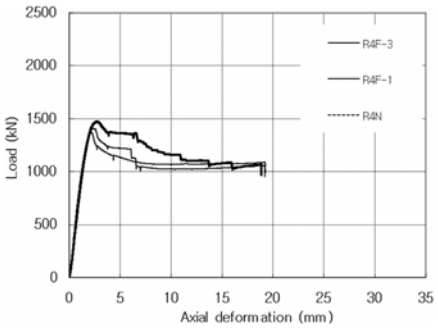

(b) Load-Displacement curves of R4 specimens

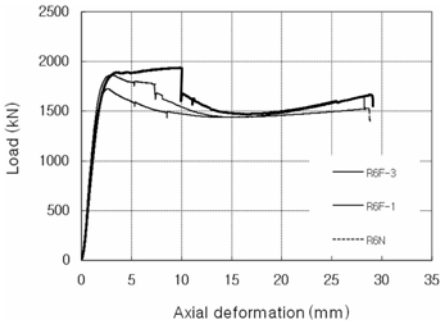

(c) Load-Displacement curves of R6 specimens

Fig. 6 Load-Displacement curves of specimens

(a) Failure shape of R6N specimen

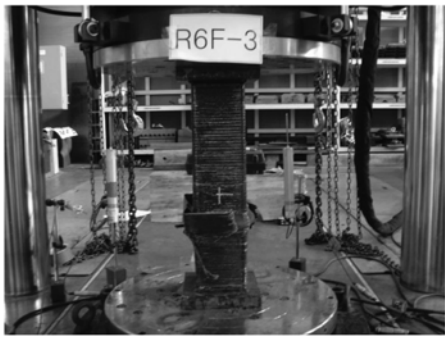

(b) Failure shape of R6F-3 specimen

Fig. 7 Specimen failure shape

The capacity of the specimens improved as width-thickness ratio decreased and the number of CFS layers increased. While the maximum strength of the specimens increased as the number of CFS layers increased, the increase in load capacity was as nominal as 6%, 7% and 12%. With the fact taken into consideration that the improvement in load capacity generated by confining effect is not experienced in CFT square columns, it was deduced that the load capacity of the columns increased though nominal because the carbon fiber sheets delayed local buckling.

From the tests, it was observed in the specimens that ductility capacity improved as the number of

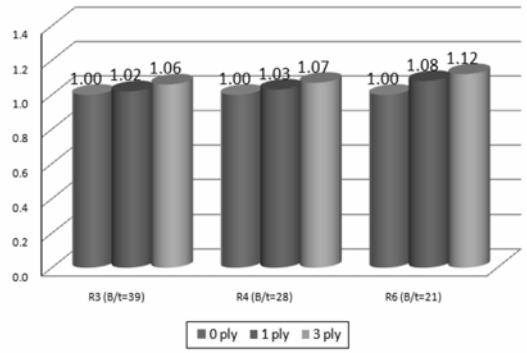

Fig. 8 The influence of the number of CFS layers on maximum strength (Column test)

Table 2 Maximum strength and ductility capacity for each specimen

Specimen	P_{max} (kN)	P_y (kN)	δ_y (mm)	P_u (kN)	δ_u (mm)	DI	Ductility improvement (%)
R3N	1285.5	1220.0	1.667	1157.0	3.133	1.879	1.00
R3F-1	1308.8	1230.0	1.580	1047.1	2.983	1.887	1.01
R3F-3	1357.0	1380.0	1.917	1221.3	4.005	2.089	1.11
R4N	1372.2	1330.0	1.500	1235.0	2.917	1.944	1.00
R4F-1	1409.3	1350.0	1.667	1268.4	3.583	2.149	1.11
R4F-3	1473.5	1400.0	1.667	1326.2	6.717	4.029	2.07
R6N	1727.3	1650.0	1.613	1554.6	6.129	3.799	1.00
R6F-1	1866.4	1800.0	1.694	1679.8	7.292	4.305	1.13
R6F-3	1936.3	1810.0	1.905	1742.7	10.017	5.258	1.38

CFS layers increased and width-thickness ratio decreased. Specimens reinforced with a carbon fiber sheet exhibited the ductility capacity similar to that of the existing CFT specimens, while those confined by three carbon fiber sheets presented the improvement in ductility capacity. As the number of CFS layers increased, the ductility capacity of the specimens (B/t=39, B/t=28 & B/t=21) improved by 11%, 107% and 38%, respectively. It was because additional confinement t by the carbon fiber sheets delayed local buckling and improved the ductility capacity of the specimens.

2.4 Summary of column test

Central axial load tests conducted for the existing CFT specimens and those confined by carbon fiber sheets with variables of width-thickness ratio and the number of CFS layers. The test results are as follows.

1) Both in the existing CFT specimens and those confined by carbon fiber sheets, columns were bent at 15~30 cm point from bottom end followed by local buckling. In the specimens reinforced by carbon fiber sheets, the sheets were ruptured by the lateral displacement of the steel tube caused by the expansion of local buckling and the specimens failed.

2) Rapid deterioration in load capacity was observed after maximum load capacity in the existing CFT specimens, while the deterioration in load capacity in those confined by carbon fiber sheets first observed at the point when the sheets were ruptured was gradual.

3) The maximum load capacity of the specimens improved as width-thickness ratio decreased and the

number of CFS layers increased. However, the improvement in maximum load capacity in CFT specimens reinforced with carbon fiber sheets was as nominal as 6~12%, showing that the number of CFS layers did not exert a great influence on the improvement of maximum load capacity. It was deduced that the maximum load capacity of CFT square columns increased though nominal as the number of CFS layers increased because the carbon fiber sheets delayed local buckling.

4) The ductility capacity of the specimens improved as the number of CFS layers increased. It was because the confining effect of the carbon fiber sheets delayed local buckling and the failure of the specimens.

3. Beam-column Test

Buildings are subject to wind load and horizontal load such as earthquake load as well as vertical load. In this study, beam-column test was carried out for the column members simplified to be under constant axial load and cyclic horizontal load. The variables of concrete strength and the number of CFS layers were used for the comparative analysis of destructive behavior, load capacity, initial stiffness and ductility capacity of the existing CFT columns and those reinforced with carbon fiber sheets.

3.1 Test plan

3.1.1 Fabrication of specimens

8 specimens were fabricated by casting concrete in square steel tubes which were 125×125×3.2, 4.5 & 6.0 (mm) in size and 550 (mm) in length. The carbon fiber sheets with the same width as the columns (125 mm) were attached to the lower part of the columns where local buckling was expected to appear. The variables for the test were the number of CFS layers and concrete strength. The design compressive strengths of the concrete were 24, 40 and 50 MPa and the numbers of CFS layers reinforcing the CFT columns were zero, one and three. Table 3 shows the details of the specimen fabrication plan.

3.1.2 Material test

The design compressive strengths of the concrete and compressive strengths (f'_c) obtained from the material test were 24, 40 and 50 MPa and 24.3, 39.9 and 53.0 MPa, respectively. The yield strength (f_y) and ultimate strength (f_u) of the steel tube were 427 MPa and 461 MPa, respectively. The design thickness and tensile strength of the carbon fiber sheets provided by the manufacturer were 0.111 mm and 3,500 MPa, respectively.

Table 3 Plan for specimens and variables (Beam-Column Test)

Specimen	Size (mm)	B/t ratio	L/B ratio	f'_c (MPa)	f_y (MPa)	CFS Layer	$A_s/A_{con'c}$ (%)	A_s (mm^2)	$A_{con'c}$ (mm^2)
R2N	125×125×3.0	28	4.4	24.3	427	0	13.88	2,169	13,456
R2F-1	125×125×3.0	28	4.4	24.3	427	1	13.88	2,169	13,456
R4N	125×125×3.0	28	4.4	39.0	427	0	13.88	2,169	13,456
R4F-1	125×125×4.5	28	4.4	39.0	427	1	13.88	2,169	13,456
R5N	125×125×4.5	28	4.4	53.0	427	0	13.88	2,169	13,456
R5F-1	125×125×4.5	28	4.4	53.0	427	1	13.88	2,169	13,456
R5F-2	125×125×6.0	28	4.4	53.0	427	2	13.88	2,169	13,456
R5F-3	125×125×6.0	28	4.4	53.0	427	3	13.88	2,169	13,456

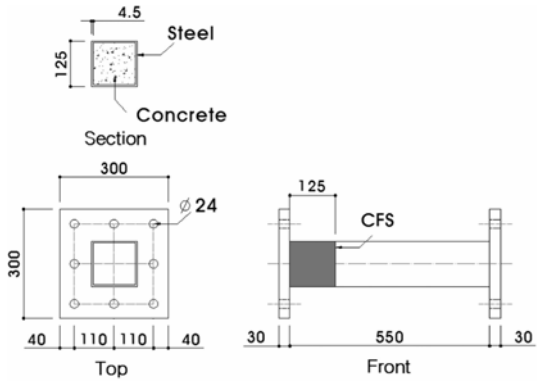

Fig. 9 Fabrication of the specimens (Beam-Column test)

3.1.3 Specimen setting

Specimens were set in order to be subject to cyclic horizontal load and central axial load simultaneously as shown in Fig. 10.

For central axial load, the 30% of the ultimate strength prescribed in the AISC/LRFD code was loaded with a 980kN oil jack. Cyclic horizontal load was also applied with a 980 kN actuator as guided in the ANSI/AISC 341-02(ANSI/AISC 2002, Yun *et al.* 2002). The peak drift ratio (Δ / L) for each cycle was 0.375%~6.0%. (Here, Δ and L mean the lateral displacement and length of the specimens, respectively.)

3.2 Specimens' failure procedures and hysteresis curves

Local buckling caused by cyclic horizontal load was observed at 7~8 cm point from the bottom end of the specimens. In CFT columns reinforced with carbon fiber sheets, the sheets were ripped and ruptured as local buckling expanded. The location of local buckling was similar to that of the existing CFT columns. As lateral load caused local buckling, carbon fiber sheets were ripped only where local buckling expanded. The sheets remained attached to steel tube in other parts. Then, the rupture of carbon fiber sheets expanded as local buckling expanded more. Carbon fiber sheets remained attached

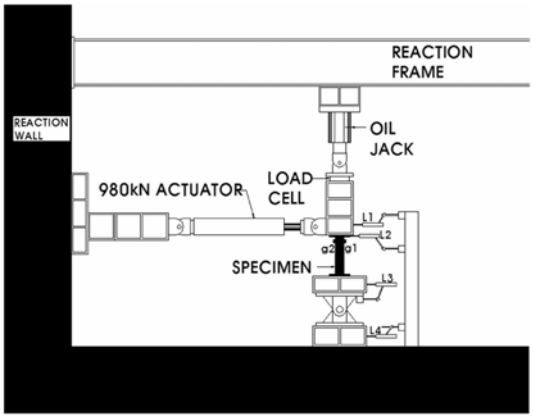

Fig. 10 Test setup (Beam-Column Test)

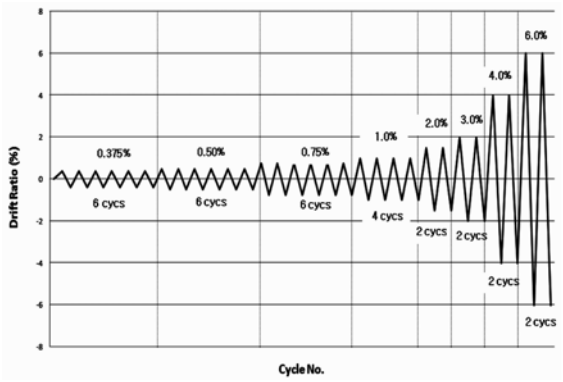

Fig. 11 Cyclic Loading Program (ANSI/ AISC 341-02)

to the steel tube where local buckling was not observed.

The failure mode procedures of the specimens for each drift ratio are as follows.

In R2N specimen (24 MPa, CFS = 0 ply), maximum moment appeared at the drift ratio of 2.0% as shown in Fig. 13 (a) and local buckling called "elephant foot" appeared at the ratio of 3.0% as shown in Fig. 13 (a). Then, local buckling expanded gradually and load capacity deteriorated. At the ratio of 4.0%, the specimen failed. In R2F-1 specimen (24 MPa, CFS = 1 ply), maximum moment appeared at the drift ratio of 2.0% as shown in Fig. 13 (b) and local buckling was observed at the ratio of 3.0% and carbon fiber sheet was ruptured shown in Fig. 13 (b). After exhibiting the expansion of buckling and deterioration in load capacity, the specimen failed at the ratio of 4.0%.

In R5N specimen (53 MPa, CFS = 0 ply), maximum moment appeared at the drift ratio of 3.0% and local buckling appeared at the second cycle of the ratio of 3.0% as shown in Fig. 13 (e). The specimen failed at the ratio of 4.0%. In R5F-1 specimen (53 MPa, CFS = 1 ply), maximum moment appeared at the drift ratio of 3.0% as shown in Fig. 13 (f) and the rupture of the carbon fiber sheet caused by local buckling was observed at the second cycle. After exhibiting the deterioration in load capacity, the specimen failed at the ratio of 4.0%.

In R5F-2 and 3 specimens (53 MPa, CFS = 2 & 3 plies), maximum moment appeared at the drift ratio of 3.0% as shown in Fig. 13 (g) and (h). Then, local buckling appeared at the drift ratio of 4.0% and the

(a) Failure shape of R5N specimen (b) Failure shape of R5F-1 specimen

Fig. 12 Failure shape of beam-column specimens

rupture of the carbon fiber sheets started. After exhibiting the expansion of local buckling and deterioration in load capacity, the specimen failed at the ratio of 6.0%. It was observed that the increase in the number of CFS layers resulted in longer delay of local buckling.

Fig. 13 shows the hysteresis curves of all specimens.

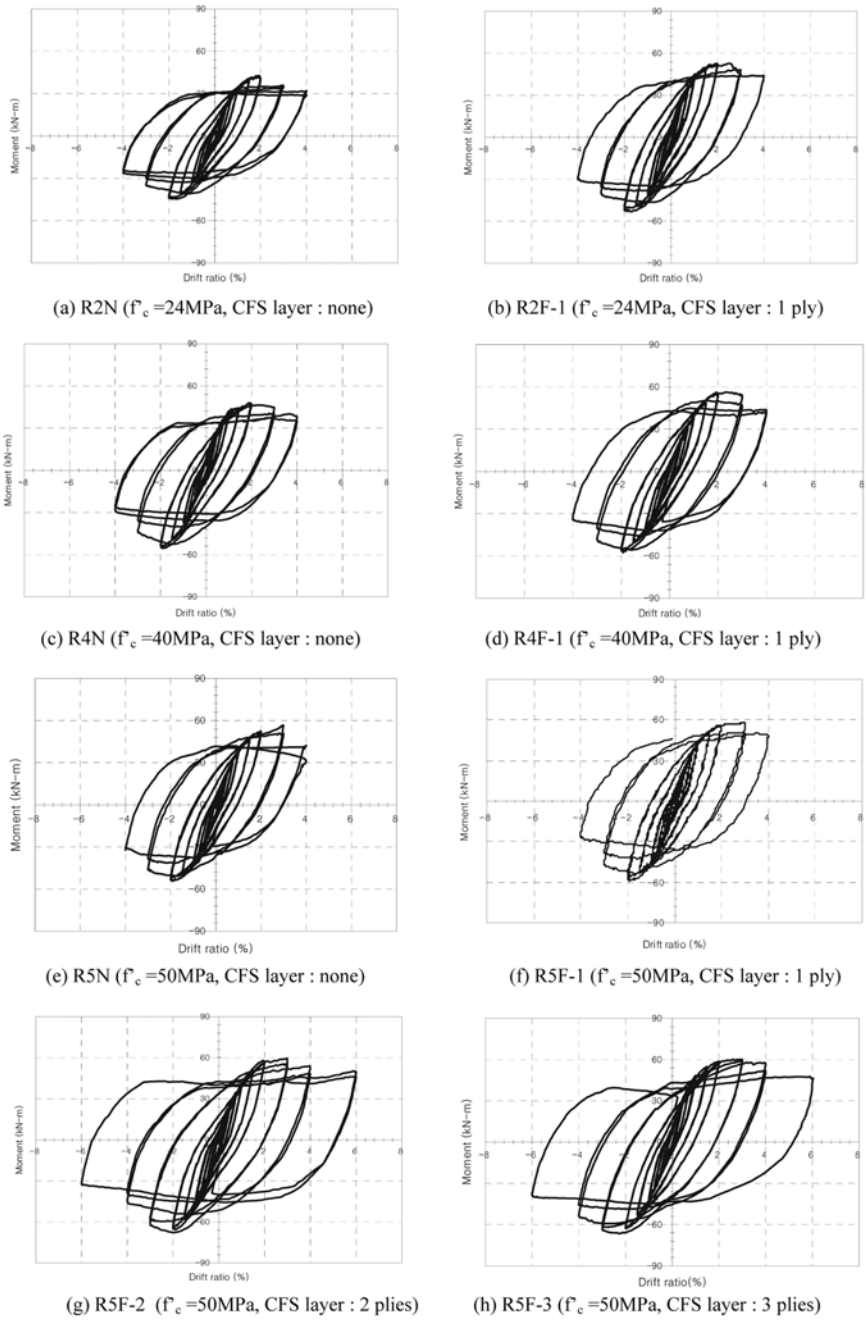

(a) R2N (f'_c =24MPa, CFS layer : none)
(b) R2F-1 (f'_c =24MPa, CFS layer : 1 ply)
(c) R4N (f'_c =40MPa, CFS layer : none)
(d) R4F-1 (f'_c =40MPa, CFS layer : 1 ply)
(e) R5N (f'_c =50MPa, CFS layer : none)
(f) R5F-1 (f'_c =50MPa, CFS layer : 1 ply)
(g) R5F-2 (f'_c =50MPa, CFS layer : 2 plies)
(h) R5F-3 (f'_c =50MPa, CFS layer : 3 plies)

Fig. 13 The hysteretic curves for specimens

3.3 Analysis of beam-column test results

Table 4 shows not only the load capacity (M_u) and drift ratio (θ_u) at failure point but also the load capacity (δ_u) and drift ratio (θ_y) at yield point. Maximum load capacity (M_{max}) and ductility (DI) are also listed in table 4. The yield point and failure point of the specimens were derived from the skeleton curve connecting the maximum moments at each drift ratios on hysteresis curve as shown in Fig. 12. Yield point was decided by the 1/3 tangent method(Choi *et al*. 2000) and failure point was defined as the point of 10% deterioration of load capacity from maximum load capacity(Varma *et al.* 2004). Ductility of the specimens is defined as Eq. (2).

$$DI = \frac{\theta_u}{\theta_y} \tag{2}$$

The averages of (+) and (-) yield points and (+) and (-) failure points were used as yield point and failure point, respectively.

3.3.1 Maximum strength and ductility

The maximum capacity of the specimens improved as concrete strength and the number of CFS layers increased. As the number of layers increased, strength of R2 specimens (f'$_c$ = 24 MPa), R4

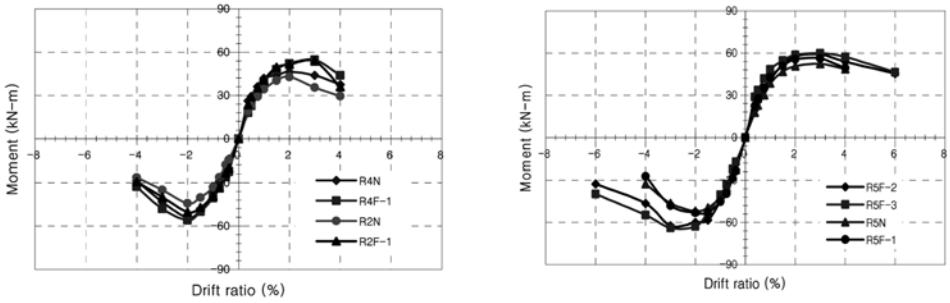

(a) Skeleton curve of specimen (f'c= 24 MPa & 40 MPa) (b) Skeleton curve of specimen (f'c= 50 MPa)

Fig. 14 Skeleton curves of specimens

Table 4 Maximum strength and ductility capacity for each specimen

Specimen	$M_{max(avg)}$ (kN-m)	$M_{y(avg)}$ (kN-m)	θ_y (%)	$M_{u(avg)}$ (kN-m)	$\theta_{u(avg)}$ (%)	DI	Ductility improvement (%)
R2N	43.48	34.6	0.801	39.2	2.55	3.18	1.00
R2F-1	44.90	36.7	0.779	40.4	2.66	3.41	1.07
R4N	50.18	38.5	0.792	45.2	2.93	3.70	1.00
R4F-1	51.20	43.8	0.844	46.1	3.35	3.96	1.07
R5N	52.21	42.4	0.855	47.0	3.38	3.95	1.00
R5F-1	53.10	44.5	0.828	47.8	3.44	4.00	1.01
R5F-2	59.20	53.0	0.878	53.3	3.82	4.34	1.10
R5F-3	61.93	53.9	0.877	55.7	4.18	4.76	1.21

specimens (f'_c = 40 MPa) and R5 specimens (f'_c = 50 MPa) increased by up to 3%, 2% and 19%, respectively (Fig. 15). It was observed that the increase in the number of the layers resulted in the increase in ultimate strength but its influence was nominal.

The ductility capacity of the specimens improved as the number of CFS layers increased as shown in Fig. 14. The specimens reinforced with a carbon fiber sheet exhibited ductility capacity similar to that of the existing CFT specimens, while those reinforced with two or three sheets (R5F-2 & 3) presented local buckling at the drift ratio of 6% and great superiority in ductility capacity to the existing CFT specimens.

For influence of concrete strength, The load capacity of the existing CFT specimens and those confined by a carbon fiber sheet improved by up to 20% and 18%, respectively as concrete strength increased, showing that increase in concrete strength led to the improvement in load capacity.

3.3.2 Peak stiffness degradation

In order to investigate stiffness degradation in the specimens under cyclic horizontal load for each cycle, maximum stiffness at each cycle on the skeleton curve was estimated. The maximum stiffness in each cycle is defined as the Eq. (3).

$$K_i = \frac{M_i}{\Delta_i} \tag{3}$$

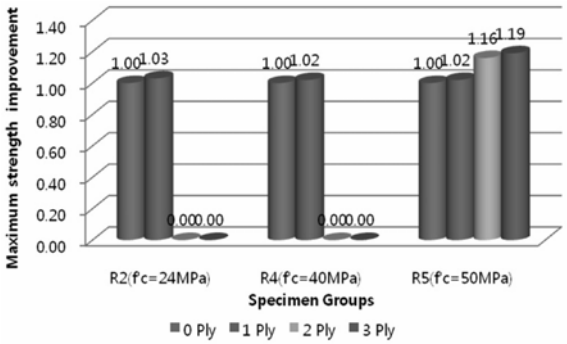

Fig. 15 The influence of the number of CFS layers on maximum strength (Beam-column test)

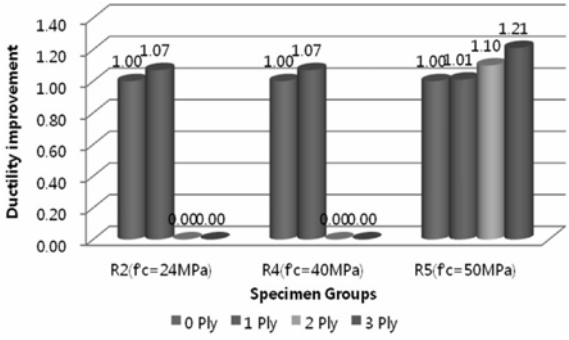

Fig. 16 The influence of the number of CFS layers on ductility (Beam-column test)

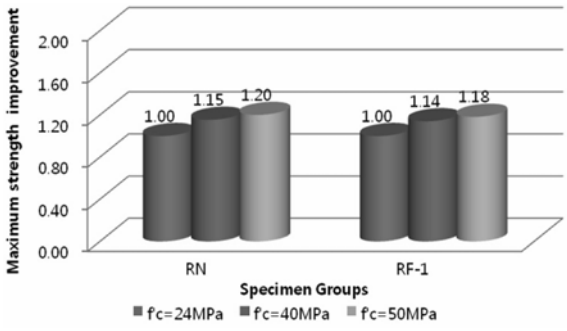

Fig. 17 The influence of concrete strength on maximum strength (Beam-column test)

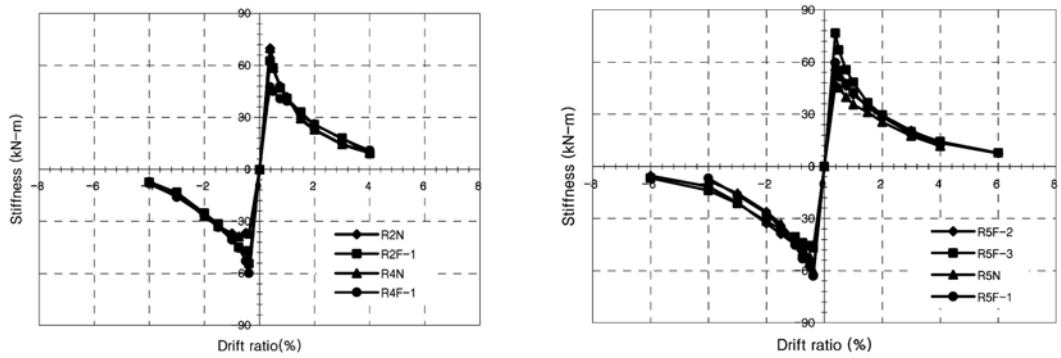

Fig. 18 The skeleton curves of stiffness degradation of specimens

Here, M_i and Δ_i mean the maximum moment and ratio in the i cycle, respectively. Fig. 19 shows the skeleton of stiffness degradation in the specimens(Mao and Xiao 2006).

As shown in Fig. 15, peak stiffness K_i increased in early drift ratios, while it decreased gradually as drift ratio increased. CFT columns reinforced with carbon fiber sheets exhibited the trend similar to that of the existing CFT columns. No difference was observed in terms of peak stiffness K_i between the two types of columns. Therefore, it was deduced that confinement by carbon fiber sheets exerted influence on the improvement in ductility capacity rather than stiffness. Consequently, it was expected that CFT structures confined by carbon fiber sheets would contribute to the improvement in seismic performance thanks to improved ductility capacity.

3.4 Summary of beam-column test result

1) CFT specimens exhibited local buckling at the 7~8 cm point from the bottom end of columns followed by failure. CFT specimens confined by carbon fiber sheets exhibited the expansion of local buckling at columns followed by the rupture of the sheets and specimen failure.

2) In CFT specimens reinforced with a carbon fiber sheet, the improvement in load capacity resulting from the sheet's confining effect was as nominal as 2~3%. In the specimens reinforced with 2 or 3 carbon fiber sheets, the improvement in load capacity ranged between 16~19%. It was deduced that the

confinement by carbon fiber sheets did not exert a great influence on the improvement in maximum load capacity.

Maximum load capacity improved by up to 20% as concrete strength increased, showing that the increase in concrete strength led to the improvement in maximum load capacity.

3) No large gap in ductility capacity was observed between CFT specimens confined by a carbon fiber sheet and the existing CFT specimens, while the specimens confined by 2 or 3 carbon fiber sheets exhibited superiority in ductility capacity to the existing CFT specimens thanks to the delay in local buckling.

4) Existing CFT specimens and those confined by carbon fiber sheets exhibited similar patterns of stiffness degradation. It was deduced that the influence of the confinement by carbon fiber sheets on the improvement in load capacity and stiffness was slighter than its influence on the delay in local buckling and improvement in ductility capacity.

4. Proposed CFT column system

4.1 Cause of strength improvement and failure mechanism

Unlike CFT circular columns, CFT square columns do not experience the improvement in concrete strength resulting from confining effect (Cai and He 2006). Thus, the load capacity of the member is usually defined as the sum of the compressive strength of concrete and that of steel tube. However, CFT square columns reinforced with carbon fiber sheets exhibited the improvement in maximum load capacity though nominal and the improvement became greater as the number of CFS layers increased.

In CFT columns reinforced with carbon fiber sheets, the confinement by the sheets delayed local buckling when the columns started to be inflated as shown in Fig. 19 (b). The sheets were ruptured as local buckling expanded and exceeded the tensile strength of the sheets. However, as shown in Fig. 19 (c), the expansion of local buckling to the area surrounding the rupture of the sheets was delayed due to the confinement by the carbon fiber sheets. The rupture of the sheets expanded as loading continued and local buckling expanded as shown in Fig. 19 (d).

With the fact taken into consideration that CFT square columns do not experience the improvement in concrete strength resulting from confining effect, it was deduced that maximum load capacity and deformation capacity improved along with the increase in the number of CFS layers because confinement by the carbon fiber sheets resulted in the improvement in strength by delaying local

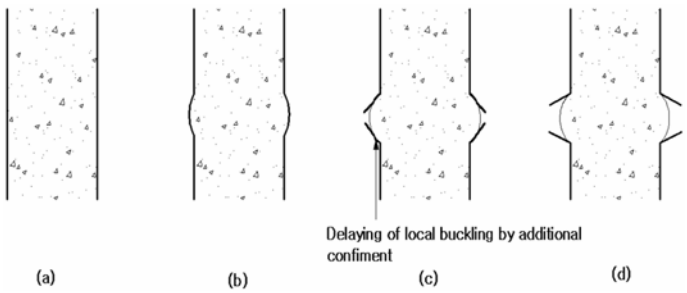

Fig. 19 Failure mechanism

buckling as shown in the Fig. 19 of failure mechanism.

4.2. Advantages of the proposed CFT system

In this study, it was observed that confinement by carbon fiber sheets could improve the capacity of existing CFT columns. The summary of the advantages associated with CFT columns confined by carbon fiber sheets is as follows.

1) Existing CFT columns resisted to the longitudinal stress caused by axial load and moment. New CFT system suggested in this study provided additional confinement in transverse direction of carbon fiber sheets and controlled or delayed the local buckling presented at potential plastic hinge area.

2) Additional confinement of the area surrounding local buckling by carbon fiber sheets did not result in the significant improvement in the load capacity and stiffness of the columns. However, the sheets delayed local buckling and led to the improvement in ductility capacity. Consequently, it was deduced that the new CFT system suggested in this study would significantly improve the seismic performance of the existing CFT system.

3) The reinforcement of CFT columns with carbon fiber sheets features advantages such as reduced term of works and building weight and invulnerability of material properties to climatic changes. Accordingly, the CFT system suggested in this study is expected to be widely used for reinforcing existing CFT buildings or bridges.

5. Conclusions

In this study, the behavior of CFT columns confined by carbon fiber sheets was analyzed to control the local buckling at CFT square columns caused by axial load and horizontal load such as earthquake load. Central axial load test and beam-column test were conducted and the behaviors of existing CFT columns and those reinforced with carbon fiber sheets were compared. The conclusion is as follows.

1) In central axial test, all the specimens were bent at 15~30 cm point from the bottom end of the column and exhibited local buckling and failure. In CFT columns reinforced with carbon fiber sheets, the sheets were ruptured due to the expansion of local buckling.

2) It was observed from central axial load test that maximum load capacity improved as width-thickness ratio decreased and the number of CFS layers increased. Though maximum strength improved as the number of CFS layers increased, the improvement in load capacity was as nominal as 6%, 7% and 12%. The confinement by carbon fiber sheets delayed local buckling and the ductility capacity of the columns increased by up to 11%~107% as the number of CFS layers increased.

3) With the fact taken into consideration that CFT square columns do not experience the improvement in concrete strength resulting from confining effect, it was deduced that maximum load capacity on load-displacement curves improved though nominal along with the increase in the number of CFS layers because the confinement by the carbon fiber sheets delayed local buckling.

4) In beam-column test, all the specimens failed after exhibiting local buckling at the lower part of columns subject to ultimate moment. In CFT columns reinforced with carbon fiber sheets, the sheets were ruptured due to the expansion of local buckling.

5) In bean-column test, while maximum load capacity increased by 3 ~ 19% as the number of CFS layers increased, the improvement in load capacity was nominal. Ductility improved by up to 21% as the number of CFS layers increased, showing that the increase in the number of layers led to the

improvement in ductility capacity.

6) The confinement by carbon fiber sheets delayed local buckling and the confining effect became obvious as the number of layers increased. Additional confinement of the area surrounding local buckling by carbon fiber sheets did not result in the significant improvement in the load capacity and stiffness of the columns. However, the new CFT system suggested in this study displayed the improvement in ductility capacity enabled by the delay in failure. Consequently, it is expected that the new CFT system confined by carbon fiber sheets will significantly improve the seismic performance of the existing CFT system and be widely used to reinforce existing CFT columns.

Acknowledgements

This study was conducted with the support of the National research laboratory project (R0A-2007-000-10047-0) funded by the Korea Science and Engineering Foundation (KOSEF) and "Development of highly-efficient production & disaster-prevention technology for skyscrapers", a Brain Korea 21 stage II project of the Korea Research Foundation. The writers of this study would like to express our heartfelt thanks for their support.

References

A. H. Varma., J. M. Ricles., R. S. Sause. and L. W. Lu., (2004) "Seismic Behavior and Design of High-Strength Square Concrete-Filled Steel Tube Beam Columns", *J. Struct. Eng,* -ASCE., **130**(2), 169-179.

AISC (2005), *Steel Construction Manual* **2**, 13th ed., American Institute of Steel Constriction .

American Concrete Institute (ACI)., (1996), *State-of art report on fiber reinforced plastic(FRP) reinforcement for concrete structures,* ACI 440R-96 Committee 440, Detroit.

ANSI/ AISC 341-02., (2002), *Seismic Provisions for Structural Steel Buildings*, 40-41.

C.S. Huang. and Y. K. Yeh., (2002), "Axial load behavior of stiffened concrete-filled steel columns", *J. Struct. Eng.* -ASCE, **128**(9), 1222-1230.

Choi. S. M., Ji. K. H. and Kim. D. K., (2000), "Evaluation on Deformation Capacity of CFT Square Columns subjected to Constant Axial and Cyclic Lateral Loads", *J. Kor. Society. Steel Construction*, **12**(2), 209-219.

H. Ge. and T. Usami., (1992), "Strength of concrete-filled thin-walled steel ox columns: Experiment", *J. Struct. Eng.* -ASCE., **118**(11), 3036-3054.

H. Saadatmanesh., M. R. Ehsani. and L. Jin., (1996) "Seismic Strengthening of Circular Bridge Pier Model with Fiber Composites", *ACI Struct. J*., **92**(3), 639-647.

J. Cai. and ZX. Q. He., (2006).,"Axial load behavior of square CFT stub column with binding bars.", *J. Construct. Steel Res.*, **62**, 472-483.

J.G. Teng., J.F. Chen., S.T. Smith. and L. Lam., (2001), FRP Strengthened RC Structures, 3-5.

J. W. Park., (2008) "Load bearing capacity for concrete filled steel square tube confined by carbon fiber sheets.", Ph.D. thesis, Honeik University, Korea.

K. Sakino. and M. Tommi., (1981),"Hysteretic behavior of concrete filled square steel tubular beam-columns failed in flexure", *Transactions. Jap. Concrete Inst.,* **3**, 439-446

Kang. C. H., Oh. Y. S. and Moon. T. S., (2001), "Strength of Axially Loaded Concrete-Filled Tubular Stub Columns", *J. Kor. Society. Steel. Construction*, **12**(2), 279-287.

S. P .Schneider.,(1998) "Axially Loaded Concrete-Filled Steel Tubes", *J. Struct. Eng.* -ASCE., **121**(10), 1125-1138

T. Fujimoto., A. Mukai., I. Nishiyama. and K. Sakino., (2004) "Behavior of Eccentrically Loaded Concrete-Filled Steel Tubular Columns", *J. Struct. Eng*., -ASCE., **130**(2), 203-212.

T. Fukumoto., (2005), "Steel-beam-to-concrete-filled-steel-tube-column Moment Connection in Japan", *Steel*

Struct., **5**, 357-365.
T. I. Lin., C.M. Huang. and S. Y. Chen.,(1993), "Concrete-filled tubular steel columns subjected to eccentric axial load", *J. Chin. Inst. Civil Hydraulic Eng.*, **5**(4), 377-386.
X.Y. Mao. and Y. Xiao (2006), "Seismic behavior of confined square CFT columns", *Eng. Struct.*, **28**(10), 1378-1386
Xiao., W. He., and K. K. Choi., (2005), "Confined Concrete-Filled Tubular Columns", *J. Struct. Eng.* -ASCE., **131**(3), 488-497.
Y. Xiao. and H. Wu., (2002) "Retrofit of Reinforced Concrete Columns Using Partially Stiffened Steel Jackets", *J. Struct. Eng.* -ASCE., **129**(6), 725-732.
Y. Xiao. and W. He., (2000) "Compressive behavior of concrete confined by carbon fiber composite jackets", *J. Mater. Civil Eng.* -ASCE., **12**(2), 139-146.
Y.S. Huang., Y. L. Long. and J. Cai., (2008), "Ultimate strength of rectangular concrete-filled steel tubular (CFT) stub columns under axial compression", *Steel and Composite Struct.,* **8**(2), 115-128.
Yun. Y. S., Kim. Y. S., Kim. J. H. and Choi. S. M., (2002), "Cyclic Testing for CFT Column-to-Bema Connections with New Diaphragm", *Second Int. Symp. Steel Struct.* 440-451.
Z. Tao., L. H. Han. and D. Y. Wang., (2008), "Strength and ductility of stiffened thin-walled hollow steel structural sub columns filled with concrete", *Thin-Wall. Struct.*, **46**(10), 1113-1128.
Z. Tao., L. H. Han. and L. L. Wang., (2007), "Compressive and flexural behavior of CFRP-repaired concrete-filled steel tubes after exposure to fire", *J. Construct. Steel. Res.*, **63**(8), 1116-1126.

CC